Available online at www.sciencedirect.com
SCIENCE DIRECT®
Journal of Sound and Vibration 272 (2004) 557–580
JOURNAL OF SOUND AND VIBRATION
www.elsevier.com/locate/jsvi

Non-linear dynamic behaviors of rolling element bearings due to surface waviness

S.P. Harsha*, K. Sandeep[1], R. Prakash

Mechanical Engineering Group, Birla Institute of Technology & Science, Pilani 333031, India

Received 11 September 2002; accepted 27 March 2003

Abstract

An analytical model to predict non-linear dynamic responses in a rotor bearing system due to surface waviness has been developed. In the analytical formulation the contacts between the rolling elements and the races are considered as non-linear springs, whose stiffness are obtained by using Hertzian elastic contact deformation theory. The governing differential equations of motion are obtained by using Lagrange's equations. The implicit type numerical integration technique Newmark-β with Newton–Raphson method is used to solve the non-linear differential equations iteratively. A computer program is developed to simulate surface waviness of the components. Results presented in the form of fast Fourier transformation with agreement of various author's experimental researches.

1. Introduction

The stiffness, rotational accuracy and vibration characteristics of a high-speed shaft are partly controlled by the ball bearings that support it. An analysis of ball bearing dynamic behavior is important to predict the system vibration responses. The behavior of non-linear systems often demonstrates unexpected behavior patterns that are extremely sensitive to initial conditions. When ball bearings are operated at high speed, they generate vibrations and noise. The principle forces, which drive these vibrations, are time varying non-linear contact forces, which exist between the various components of the bearings: rolling elements, races and shafts. In the shaft bearing assembly supported by rolling element bearings, the vibration spectrum is dominated by

*Corresponding author. Tel.: +91-1596-242210; fax: +91-1596-244183.
E-mail addresses: suraj@bits-pilani.ac.in (S.P. Harsha), sandeepkumar333@hotmail.com (K. Sandeep), rprakash@bits-pilani.ac.in (R. Prakash).
[1] Asian Institute of Medicine, Science & Technology, Malaysia.

0022-460X/03/$ - see front matter © 2003 Elsevier Ltd. All rights reserved.
doi:10.1016/S0022-460X(03)00384-5

the vibrations at the natural frequency and the ball passage frequency (BPF). The vibrations at this later frequency are called ball passage vibrations (BPV).

The vibrations are also generated by geometrical imperfections on the individual bearing components and these imperfections are caused by irregularities during the manufacturing process. Although the amplitude of these imperfections are on micrometer scale, but they can still produce significant vibrations in the applications. The imperfection such as surface waviness in the rolling elements and races developed during manufacturing process, produce significant vibrations in the system. The radial and axial clearances, which provided in the design of bearing to compensate the thermal expansion, are also a source of vibrations and introduce the non-linearity in the dynamic behavior.

The early work done in the rotor dynamics by Yamamoto [1] investigate analytically the vibration characteristics of vertical rotors supported by ball bearings with the effect of bearing radial clearances. The conclusion of this work shows that the maximum amplitude at critical speed as well as the value of the critical speed decreases with increasing radial clearances and critical speed disappears under the condition beyond a marginal clearance, which depends on the amount of unbalance. Gustafson et al. [2] studied the effects of waviness and pointed out that lower order ring waviness affects the amplitude of the vibrations at the BPF. They observed that vibrations at higher harmonics of the BPF are also present in the vibration spectrum and their amplitudes depend on the radial load, radial clearance, rotational speed and the order of harmonics. The same conclusion was theoretically proved by Meyer et al. [3] for perfect radial ball bearings with linear modelling of the spring characteristics of balls. Gad et al. [4] showed that resonance occurs when BPF coincides with frequency of the system and they also pointed out that for certain speeds, BPF can exhibit its sub and super harmonic vibrations for shaft ball bearing system.

El-Sayed [5] derived a form of equation for the stiffness of bearings and determined total deflections of inner and outer races caused by an applied load, using the Hertz theory. Tamura and Tsuda [6] performed a theoretical study of fluctuations of the radial spring characteristics of a ball bearing due to ball revolutions. Bal 'Mont et al. [7] considered two factors for structural vibrations of ball bearings, one of these is the contact load from the balls, which deform the races into polyhedral shape, and other is the motion of balls relative to the line of action of the radial load which fluctuates the rigidity of the bearing.

Sayles and Poon [8] found that the waviness causes most of the sever vibrations and noise problems in the bearings. They reported that waviness produces vibrations at frequencies up to approximately 300 times the rotational speed but is predominant at frequencies at below about 60 times rotational speeds. Datta and Farhang [9] developed a non-linear model for structural vibrations in the rolling bearings by considering the stiffness of the individual region where the elements contact each other but in this model distributed defects are not considered. Wardle and Poon [10] also pointed out the relations between the number of balls and waves for sever vibrations to occur. When the number of balls and waves are equal there would be severing vibrations. Yhland [11] presented a linear theory of vibrations of shaft bearing system caused by ball bearing geometrical imperfections.

Aktürk [12] presented the effect of surface waviness on vibrations associated with ball bearings and conclude that for outer race waviness most sever vibrations occur when the BPF and its harmonics coincide with the natural frequency. Aktürk et al. [13] performed a theoretical

investigations of effect of varying the preload on the vibration characteristics of a shaft bearing system and also suggested that by taking correct number of balls and amount of preload in a bearing untoward effect of the BPV can be reduced. Wardle [14] showed that in case of inner race waviness, the axial vibrations take place at frequencies harmonic with ball to inner race passage rate N_b $(\omega - \omega_c)$ and the ball waviness produced vibrations in the axial and radial directions at different frequencies and also pointed out that only even orders of ball waviness produced vibrations.

It is well known that the surface waviness of the races and non-linear restoring force at each contact point have vital role in dynamics of the bearings. In this paper, a theoretical investigation was made to observe the effect of surface waviness on the vibration characteristics of a rotor bearing system. A 3-d.o.f. system is considered with the assumption that there is no friction between the balls and raceways and that both bearings are positioned symmetrically such that their moving parts are in synchronization. Fast Fourier transformations are obtained to study the non-linear dynamic responses of rolling element bearings.

2. The problem formulation

A schematic diagram of rolling element bearing is shown in Fig. 1. For investigating the structural vibration characteristics of rolling element bearing, a model of bearing assembly can be considered as a spring–mass system, in which the outer race of the bearing is fixed in a rigid support and the inner race is fixed rigidly with the shaft. Elastic deformation between races and rollers give a non-linear force deformation relation, which is obtained by Hertzian theory. Other sources of stiffness variation are positive internal radial clearance, finite number of balls whose position changes periodically and the inner and outer race waviness. These cause periodic changes in stiffness of bearing assembly. Thus, the system undergoes non-linear vibration under dynamic conditions.

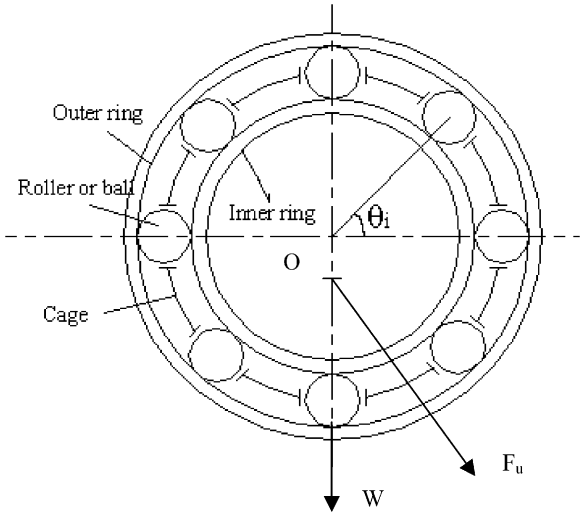

Fig. 1. A schematic diagram of a rolling element bearing.

In the mathematical modelling, the rolling element bearing is considered as spring–mass system and rolling elements act as non-linear contact spring as shown in Fig. 2. Since the Hertzian forces arise only when there is contact deformation, the springs are required to act only in compression. In other words, the respective spring force comes into play when the instantaneous spring length is shorter than its unstressed length, otherwise the separation between rolling element and the races takes place and the resultant force is set to zero.

2.1. Race waviness

An important source of vibrations in ball bearings is waviness. These are global sinusoidal shaped imperfections on the outer surface of the bearing Components as shown in Fig. 3a. The characteristic wavelengths of the imperfections are much larger than the dimensions of the Hertzian contact areas between the balls and the guiding races. The number of waves per circumference is denoted by the wave number. Waviness imperfections cause variations in the contact loads when the bearing is running. The magnitude of the variation depends on the amplitude of the imperfection and the non-linear stiffness in the contact. Due to the variations in the contact loads, vibrations are generated in the bearing. Imperfections with a different wave number cause vibrations at distinct frequencies, each with a characteristic vibration mode. The surface waviness in bearing causes additional vibrations.

Waviness is in the form of peaks and valleys of varying height and width. Therefore, for mathematical modelling using waviness effect, a statistical approach is necessary in order to have complete solution. If the rings are assumed to bend due to rolling element loads then the flexural vibrations of the rings as well as the rigid body motion have to be considered. To avoid these problems the inner and outer rings are assumed not to bend under these loads and a sinusoidal

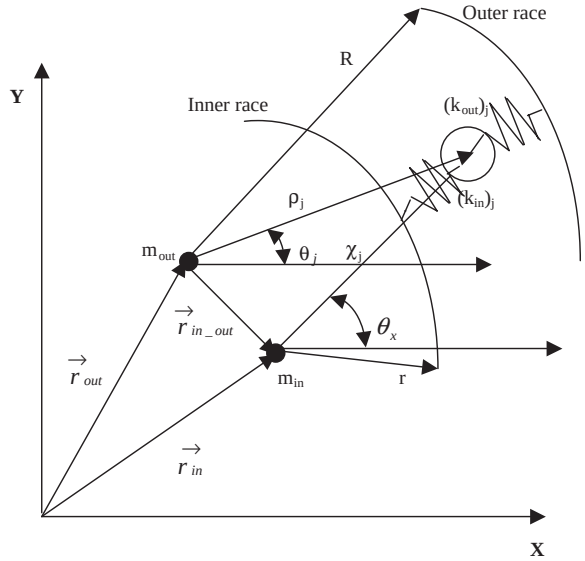

Fig. 2. Mass–spring model of the rolling element bearing.

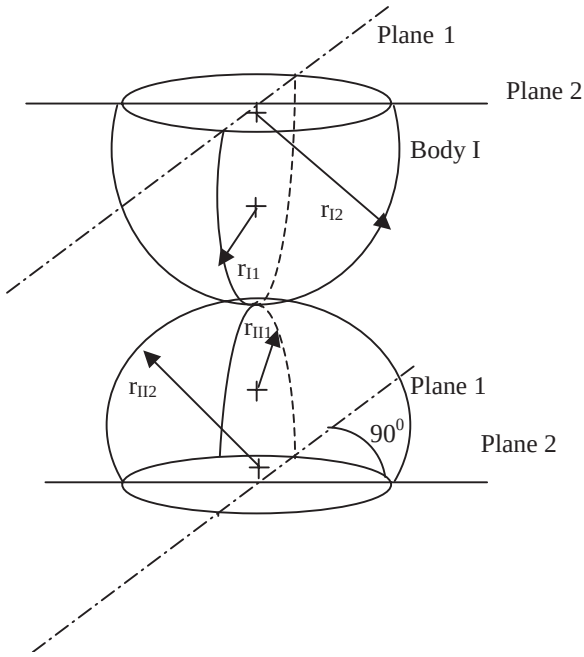

Fig. 3. Geometry of contacting bodies.

wavy surface is assumed. The wavelength is assumed to be much greater than the ball to race foot print width and the wave geometry itself is assumed to be unaffected by contact distortion. Waves are described in terms of two parameters: the wavelength (λ), which is the distance taken by a single cycle of the wave and its amplitude (Π).

2.1.1. Inner race waviness

When the rolling element is moving round the inner race, it follows the rolling surface contours continuously. It is assumed that no slip condition, i.e. rolling element always in contact with inner race and also it is assumed that the inner race surface has a circumferential sinusoidal wavy feature. The amplitude of wavy surface is often with respect to central point at a certain angle from the reference axis. Hence the amplitude of sinusoidal wave is

$$\Pi = \Pi_o \sin\left(2\pi\frac{L}{\lambda}\right). \tag{1}$$

The inner race has circumference sinusoidal wavy surface, therefore, the radial clearance consist of a constant part and a variable part. Hence the amplitude of the wave of inner race is

$$(\Pi)_{in} = (\Pi_O) + (\Pi_p)\sin\left(2\pi\frac{L}{\lambda}\right), \tag{2}$$

where Π_p is the maximum amplitude of wave and Π_o is initial wave amplitude (or constant clearance) as shown in Fig. 3b.

The arc length (L) of the wave of inner race at the contact angle is

$$L = r\theta_j. \tag{3}$$

For an imperfect surface with N waves, the wavelength (λ) is inversely proportional to the number of waves N as

$$\lambda \propto \frac{1}{N}. \tag{4}$$

For the inner race the wavelength is ratio of length of the inner race circumference to the number of waves on circumference.

$$\lambda = \frac{2r\pi}{N}, \tag{5}$$

where r is radius of inner race.

The amplitude of the waves of inner race at the contact angle is

$$(\Pi)_{in} = (\Pi_O) + (\Pi_p)\sin(N\theta_j), \tag{6}$$

where θ_j is the contact angle of jth rolling element. Since the inner race is moving at the speed of shaft and ball center is at the speed of the cage. After time taken 't', the cage will lag the shaft, so ball center will lag the inner race. Hence the contact angle is

$$\theta_j = \frac{2\pi}{N_b}(j-1) + (\omega_{cage} - \omega) \times t, \tag{7}$$

where N_b is the number of rolling element, t is the time co-ordinate.

$$j = 1, 2, 3, \ldots, N_b,$$

where

$$\omega_{cage} = \frac{1}{2}\omega_{inner}\left[1 - \frac{\rho_j}{R_p}\right] + \frac{1}{2}\omega_{outer}\left[1 + \frac{\rho_j}{R_p}\right], \tag{8}$$

where R_p is the pitch radius.

2.1.2. Outer race waviness

The outer race surface also has circumferential sinusoidal wavy surface, and the outer race is assumed to be stationary, hence both outer race and rolling element are rotating at the speed of cage. The amplitude of sinusoidal wave of outer race is

$$\Pi = \Pi_o \sin\left(2\pi \frac{L'}{\lambda'}\right). \tag{9}$$

The arc length (L') of the wave of outer race at the contact angle is

$$L' = R\theta_j. \tag{10}$$

For the outer race the wavelength is ratio of length of the inner race circumference to the number of waves on circumference.

$$\lambda' = \frac{2R\pi}{N}, \tag{11}$$

where R is radius of inner race.

Hence the amplitude of the wave of outer race is

$$(\Pi)_{out} = (\Pi_O) + (\Pi_p)\sin(N\theta_j). \tag{12}$$

Hence the contact angle is

$$\theta_j = \frac{2\pi}{N_b}(j-1) + \omega_{cage} \times t. \tag{13}$$

For a rolling element at an angular position θ_j, the inner race contact point will be at $[r + (\Pi)_{in}]$ and for this rolling element the outer race contact point will be at $[R - (\Pi)_{out}]$. From bearing geometry:

$$[R - (\Pi)_{out}] - [r + (\Pi)_{in}] = 2(\rho_r), \tag{14}$$

where ρ_r is the radius of rolling element.

2.2. Contact stiffness

Hertz considered the stress and deformation in the perfectly smooth, ellipsoidal, contacting elastic solids. The application of the classical theory of elasticity to the problem forms the basis of stress calculation for machine elements as ball and roller bearings. Therefore, the point contact between the race and ball develop into an area contact which has the shape of an ellipse with a and b as the semi-major and semi-minor axes, respectively. The curvature sum and difference are needed in order to obtain the contact force of the ball. The curvature sum $\sum \rho$ is obtained as from Harris [15] is expressed as

$$\sum \rho = \rho_{I1} + \rho_{I2} + \rho_{II1} + \rho_{II2} = \frac{1}{r_{I1}} + \frac{1}{r_{I2}} + \frac{1}{r_{II1}} + \frac{1}{r_{II2}}. \tag{15}$$

The curvature $F(\rho)$ difference is expressed as

$$F(\rho) = \frac{(\rho_{I1} - \rho_{I2}) + (\rho_{II1} - \rho_{II2})}{\sum \rho}. \tag{16}$$

The parameters $r_{I1}, r_{I2}, r_{II1}, r_{II2}, \rho_{I1}, \rho_{I2}, \rho_{II1}, \rho_{II2}$ are dependent upon calculations referring to the inner and outer races as shown in Fig. 3. If the inner race is considered,

$$r_{I1} = \frac{D}{2}, r_{I2} = \frac{D}{2}, r_{II1} = \frac{d_i}{2}, r_{II2} = r_i$$

and

$$\rho_{I1} = \frac{2}{D}, \rho_{I2} = \frac{2}{D}, \rho_{II1} = \frac{2}{d_i}, \rho_{II2} = -\frac{1}{r_i}. \tag{17}$$

If outer race is considered, they are given as

$$r_{I1} = \frac{D}{2}, r_{I2} = \frac{D}{2}, r_{II1} = \frac{d_o}{2}, r_{II2} = r_o$$

and

$$\rho_{I1} = \frac{2}{D}, \rho_{I2} = \frac{2}{D}, \rho_{II1} = -\frac{2}{d_o}, \rho_{II2} = -\frac{1}{r_o}. \tag{18}$$

As per the sign convention followed, negative radius denotes a concave surface. Using Table 2 calculation of all the parameters including curvature difference at inner and outer race can be done. For the contacting bodies being made of steel, the relative approach between two contacting and deforming surface is given by

$$\delta = 2.787 \times 10^{-8} Q^{2/3} \left(\sum \rho\right)^{1/3} \delta^*, \tag{19}$$

where δ^* is a function of $F(\rho)$.

Hence, the contact force (Q) is

$$Q = \{3.587 \times 10^7 \left(\sum \rho\right)^{1/2} (\delta^*)^{-3/2}\} \delta^{3/2} (\mathrm{N}). \tag{20}$$

The elastic modulus for the contact of a ball with the inner race is

$$K_i = 3.587 \times 10^7 \left(\sum \rho_i\right)^{-1/2} (\delta_i^*)^{-3/2} \left(\frac{\mathrm{N}}{\mathrm{mm}}\right). \tag{21}$$

And for the contact of a ball with the outer race is

$$K_o = 3.587 \times 10^7 \left(\sum \rho_o\right)^{-1/2} (\delta_o^*)^{-3/2} \left(\frac{\mathrm{N}}{\mathrm{mm}}\right). \tag{22}$$

Then the effective elastic modulus K for the bearing system is written as

$$K = \frac{1}{\left(1/K_i^{1/n} + 1/K_o^{1/n}\right)^n}. \tag{23}$$

In Eqs. (21) and (22), the parameters δ_i^* and δ_o^* can be attained from Table 1, if the values of $F(\rho)_i$ and $F(\rho)_o$ are available with using of Table 2. The effective elastic modulus (K) for bearing system with using geometrical and physical parameters is written as

$$K = 7.055 \times 10^5 \sqrt{\delta} \frac{\mathrm{N}}{\mathrm{mm}}. \tag{24}$$

2.3. Derivation of governing equations of motion

A model for analysis of non-linear dynamic response due to distributed defects of rolling element bearings is developed. First the expressions for kinetic and potential energies are formulated for all components of rolling element bearing. Utilizing Lagrange's equations with using these energies expression can derive the equations of motion that describe the dynamic behavior of complex model. A real shaft-rolling bearing system is generally very complicated and difficult to model, so following assumptions are made in the development of the mathematical model.

Table 1
Dimensional contact parameters

F (ρ)	δ
0	1
0.1075	0.997
0.3204	0.9761
0.4795	0.9429
0.5916	0.9077
0.6716	0.8733
0.7332	0.8394
0.7948	0.7961
0.83595	0.7602
0.87366	0.7169
0.90999	0.6636
0.93657	0.6112
0.95738	0.5551
0.97290	0.4960
0.983797	0.4352
0.990902	0.3745
0.995112	3176
0.997300	0.2705
0.9981847	0.2427
0.9989156	0.2106
0.9994785	0.17167
0.9998527	0.11995
1	0

Table 2
Geometric and physical properties used for the rolling element bearings

Mass of rolling element (m_j)	0.009 kg
Mass of the inner race (m_{in})	0.06 kg
Mass of the outer race (m_{out})	0.065 kg
Mass of the shaft (m_s)	5.5 kg
Radius of inner race with point of contact with the rolling element (r)	23 mm
Radius of outer race with point of contact with the rolling element (R)	31 mm
Radius of each rolling element (ρ_j)	3.98 mm
Radial load (W)	10 N
Pitch radius of ball set	2.7 mm
Angular velocity of inner race (ϕ_{in})	2500 rpm
Maximum amplitude of waviness (Π_p)	2 μm
Initial amplitude of waviness (Πo)	1 μm
Initial radial position of jth rolling element (ρ_j)	27 mm
Initial position of center of inner race (x_{in}, y_{in})	(0, 0) mm
Initial position of center of inner race (x_{out}, y_{out})	(0, 0) mm

1. Deformations occur according to the Hertzian theory of elasticity. Hence only small elastic motions of the rolling elements and the rings are considered.
2. The rolling elements, the inner and outer races and the shaft have motions in the plane of bearing only.
3. The angular velocity of the cage is assumed to be constant.
4. The rollers in a rolling bearing are assumed to have no angular rotation about their axes. Hence there is no interaction of the corners of the rollers with the cage and the flanges of the races.
5. All the bearing components and the rotor are rigid.
6. The outer race is rigid to the support and the inner race is fixed rigidly to the shaft, i.e. there is no bending.
7. The cage ensures the constant angular separation (β) between rolling elements, hence there is no interaction between rolling elements. Hence,

$$\beta = \frac{2\pi}{N_b}. \tag{25}$$

To obtain the equations of motion of the bearing system, the Lagrange's equation for a set of independent generalized co-ordinates:

$$\frac{\mathrm{d}}{\mathrm{d}t}\frac{\partial T}{\partial\{\dot{p}\}} - \frac{\partial T}{\partial\{p\}} + \frac{\partial V}{\partial\{p\}} = \{f\}, \tag{26}$$

where the T, V, p and f are kinetic energy, potential energy, vector with generalized d.o.f. co-ordinate and vector with generalized contact forces, respectively. The kinetic and potential energies can be subdivided into the contributions from the various components, i.e. from the rolling elements, the inner race, the outer race and the shaft.

The total kinetic energy of the bearing system is the sum of the rolling elements, inner and outer races and the shaft:

$$T = \sum_{j=1}^{N_b} T_{roller} + T_{i\_race} + T_{o\_race} + T_{shaft}. \tag{27}$$

The subscripts *i_race*, *o_race* and shaft refer to, respectively, the inner race, the outer race and the shaft. The subscript roller indicates the rolling elements and the other subscript j refers to the element under consideration.

The potential energy is provided by deformations of the balls with the races and deformations occur according to Hertzian contact theory of elasticity. Potential energy formulation is performed taking datum as the horizontal plane through the global origin. The total potential energy of the bearing system is the sum of the balls, inner and outer races, springs and the shaft:

$$V = \sum_{j=1}^{N_b} V_{roller} + V_{i\_race} + V_{o\_race} + V_{springs} + V_{shaft}, \tag{28}$$

where V_{roller}, V_{i_race}, V_{o_race} and V_{shaft} are the potential energies due to elevation of the rolling element, inner and outer races and the shaft, respectively. $V_{springs}$ is potential energy due to non-linear spring contacts between balls and the races.

2.3.1. Contribution of the inner race

Apart from local deformations in the contacts, the inner race is considered as a rigid body. The kinetic energy of the inner race about its center of mass is evaluated in x- and y-frame. The position of the origin of the moving frame relative to the reference frame is described by transitional d.o.f. $\dot{x}_{in}$ and $\dot{y}_{in}$.

The kinetic energy expression for the inner race is

$$T_{i\_race} = \tfrac{1}{2} m_{in} (\vec{r}_{in} \cdot \vec{r}_{in}) + \tfrac{1}{2} I_{in} \dot{\phi}_{in}^2. \tag{29}$$

The position of inner race center is defined with respect to the outer race center. The x_{in} and y_{in} co-ordinates are defined with respect to outer race center. The displacement vector showing the location of inner race center with respect to outer race center is

$$\vec{r}_{in} = \vec{r}_{out} + \vec{r}_{in\_out} \tag{30}$$

or

$$\vec{r}_{in} = (\vec{x}_{in} + \vec{x}_{out})\hat{i} + (\vec{y}_{in} + \vec{y}_{out})\hat{j}. \tag{31}$$

Differentiation of r_{in} with respect to time (t) gives

$$\dot{r}_{in} = (\dot{x}_{in}\vec{i} + \dot{y}_{in}\vec{j}). \tag{32}$$

$\dot{x}_{out}$ and $\dot{y}_{out}$ are zero because of the outer race is assumed to be stationary.

Hence,

$$T_{i\_race} = \tfrac{1}{2} m_{in} (\dot{x}_{in}^2 + \dot{y}_{in}^2) + \tfrac{1}{2} I_{in} \dot{\phi}_{in}^2. \tag{33}$$

The position of the inner race is defined from the outer race center, hence the potential energy for the inner race is

$$V_{i\_race} = m_{in} g (y_{in} + y_{out}). \tag{34}$$

2.3.2. Contribution of the outer race

The outer race is also considered as a rigid body and it is assumed that the outer race is stationary. Hence, $\dot{r}_{out} = 0$ and $\dot{\phi}_{out} = 0$.

The kinetic energy expression for the outer race is

$$T_{o\_race} = \tfrac{1}{2} m_{out} (\dot{\vec{r}}_{out} \cdot \dot{\vec{r}}_{out}) + \tfrac{1}{2} I_{out} \dot{\phi}_{out}^2 = 0. \tag{35}$$

The potential energy of the outer race is

$$V_{o\_race} = m_{out} g y_{out}. \tag{36}$$

2.3.3. Contribution of the rolling elements

The rolling elements are also considered as rigid bodies. For the determination of their contribution to the kinetic energy, the position of the jth-rolling element is described by two transitional d.o.f., $(\dot{\rho}_j + \dot{r}_{out})$ and $\dot{\phi}_j$.

The kinetic energy due to the rolling elements to be obtained as a summation of those from each element as

$$T_{roller} = \sum_{j=1}^{N_b} T_j. \tag{37}$$

The position of the center of ball is defined with respect to the outer race center. Hence, the kinetic energy of the jth rolling element be written as

$$T_j = \tfrac{1}{2} m_j (\dot{\vec{\rho}}_j + \dot{\vec{r}}_{out})(\dot{\vec{\rho}}_j + \dot{\vec{r}}_{out}) + \tfrac{1}{2} I_j \dot{\phi}_j^2. \tag{38}$$

The displacement vector showing the location of jth rolling elements is

$$\vec{\rho}_j = (\vec{\rho}_j \cos\theta_j)\,\hat{i} + (\vec{\rho}_j \sin\theta_j)\hat{j}. \tag{39}$$

And for the outer race center is

$$\vec{r}_{out} = \vec{x}_{out}\hat{i} + \vec{y}_{out}\hat{j}. \tag{40}$$

Differentiate Eqs. (39) and (40) with respect to time (t) and after summation, we get

$$\begin{aligned}(\dot{\vec{\rho}}_j + \dot{\vec{r}}_{out})\,(\dot{\vec{\rho}}_j + \dot{\vec{r}}_{out}) &= \dot{\rho}_j^2 \cos^2\theta_j \\ &+ \rho_j^2 \sin^2\theta_j \dot{\theta}_j^2 - 2\dot{\rho}_j \rho_j \dot{\theta}_j \cos\theta_j \sin\theta_j + \dot{x}_{out}^2 \\ &+ 2\dot{x}_{out}(\dot{\rho}_j \cos\theta_j - \rho_j \sin\theta_j \dot{\theta}_j) + \dot{\rho}_j^2 \sin^2\theta_j \\ &+ \rho_j^2 \cos^2\theta_j \dot{\theta}_j^2 + 2\dot{\rho}_j \rho_j \dot{\theta}_j \cos\theta_j \sin\theta_j \\ &+ \dot{y}_{out}^2 + 2\dot{y}_{out}(\dot{\rho}_j \sin\theta_j + \rho_j \cos\theta_j \dot{\theta}_j).\end{aligned} \tag{41}$$

The outer race is assumed to be constant, hence $\dot{x}_{out} = 0$ and $\dot{y}_{out} = 0$.

$$\begin{aligned}(\dot{\vec{\rho}}_j + \dot{\vec{r}}_{out})\,(\dot{\vec{\rho}}_j + \dot{\vec{r}}_{out}) &= \dot{\rho}_j^2 \cos^2\theta_j + \rho_j^2 \sin^2\theta_j \dot{\theta}_j^2 \\ &+ \dot{\rho}_j^2 \sin^2\theta_j + \rho_j^2 \cos^2\theta_j \dot{\theta}_j^2\end{aligned} \tag{42}$$

or

$$(\dot{\vec{\rho}}_j + \dot{\vec{r}}_{out})\,(\dot{\vec{\rho}}_j + \dot{\vec{r}}_{out}) = (\dot{\rho}_j^2 + \rho_j^2 \dot{\theta}_j^2). \tag{43}$$

From Eq. (37), we get

$$T_j = \tfrac{1}{2} m_j (\dot{\rho}_j^2 + \rho_j^2 \dot{\theta}_j^2) + \tfrac{1}{2} I_j \dot{\phi}_j^2. \tag{44}$$

It is assumed that there is no slip, hence the relative transitional velocity of outer race and ball must be same and in reverse direction. Therefore, the contact equation for jth ball and the outer race can be written as

$$R(\dot{\phi}_{out} - \dot{\theta}_j) = -\rho_r(\dot{\phi}_j - \dot{\theta}_j). \tag{45}$$

The outer race is stationary, hence

$$\dot{\phi}_{out} = 0 \tag{46}$$

or

$$\dot{\phi}_j = \dot{\theta}_j\left(1 + \frac{R}{\rho_r}\right). \tag{47}$$

Now the kinetic energy of the jth ball be written as

$$T_{ball} = \sum_{j=1}^{N_b} \frac{1}{2} m_j(\dot{\rho}_j^2 + \rho_j^2\dot{\theta}_j^2) + \frac{1}{2} I_j\dot{\theta}_j^2\left(1 + \frac{R}{\rho_r}\right)^2. \tag{48}$$

For the balls, the potential energy due to elevation is

$$V_{ball} = \sum_{j=1}^{N_b} m_j g(\rho_j \sin\theta_j + y_{out}) \tag{49}$$

or

$$V_{ball} = \sum_{j=1}^{N_b} m_j g\rho_j \sin\theta_j + mgN_b y_{out}. \tag{50}$$

2.3.4. Contribution of the shaft

The kinetic energy of the shaft is calculated by assuming that its center remains coincident with the inner race. Hence, the kinetic energy of the shaft is

$$T_{shaft} = \tfrac{1}{2} m_s(\dot{x}_{in}^2 + \dot{y}_{in}^2) + \tfrac{1}{2} I_s\dot{\theta}_s^2. \tag{51}$$

The shaft center is coinciding with inner race center and position of the inner race center is defined with respect to outer race center. Hence, the potential energy of the shaft is expressed as

$$V_{shaft} = m_s g(y_{in} + y_{out}). \tag{52}$$

2.3.5. Contribution of the contact deformation

The contacts between balls and races treated as non-linear springs, whose stiffness obtained by Hertzian theory of elasticity. The expression of potential energy due to the contact deformation of the springs is

$$V_{spring} = \sum_{j=1}^{N_b} \frac{1}{2} k_{in}\delta_{in}^2 + \sum_{j=1}^{N_b} \frac{1}{2} k_{out}\delta_{out}^2, \tag{53}$$

where k_{in} and k_{out} are the non-linear stiffness due to Hertzian contact effects.

The deformation at contact points between the jth rolling element and inner race is

$$\delta_{in} = \lfloor\{r + \rho_r\} - \chi_j\rfloor. \tag{54}$$

In this expression, if $\{r + \rho_r\} > \chi_j$, compression takes place and restoring force act.

If $\{r + \rho_r\} < \chi_j$, no compression and restoring force is set to zero. Similarly, at the outer race the deformation at the contact points is

$$\delta_{out} = \left\lfloor R - \{\rho_j + \rho_r\}\right\rfloor. \tag{55}$$

In this expression, if $R < \{\rho_j + \rho_r\}$, compression takes place and restoring force act.

If $R > \{\rho_j + \rho_r\}$, no compression and restoring force is set to zero.

2.4. Equations of motion

The kinetic energy and potential energy contributed by the inner race, outer race, balls, shaft and springs, can be differentiated with respect to the generalized co-ordinates ρ_j ($j = 1, 2, \ldots, N_b$), x_{in}, and y_{in} to obtain the equations of motion. For the generalized co-ordinates ρ_j, where $j = 1, 2, \ldots, N_b$, the equations are

$$\begin{aligned} &m_j\ddot{\rho}_j + m_j g \sin\theta_j + m_j\rho_j\dot{\theta}^2 - (k_{in}) \\ &\times [(r+\rho_r) - \chi_j]_+ \frac{\partial\chi_j}{\partial\rho_j} + (k_{out})[R - (\rho_j + \rho_r)]_+ \\ &\times + \frac{1}{2}\frac{\partial k_{in}}{\partial\rho_j}[(r+\rho_r) - \chi_j]_+^2 + \frac{1}{2}\frac{\partial k_{out}}{\partial\rho_j} \\ &\times [R - (\rho_j + \rho_r)]_+^2 = 0, \quad j = 1, 2, \ldots, N_b. \end{aligned} \tag{56}$$

For the generalized co-ordinate x_{in} the equation is

$$(m_{in} + m_s)\ddot{x}_{in} - \sum_{j=1}^{N_b} k_{in}[(r+\rho_r) - \chi_j]_+ \frac{\partial\chi_j}{\partial x_{in}} = F_u \sin(\omega t). \tag{57}$$

For the generalized co-ordinate y_{in} the equation is

$$(m_{in} + m_s)\ddot{y}_{in} + (m_{in} + m_s)g - \sum_{j=1}^{N_b} k_{in}[(r+\rho_r) - \chi_j]_+ \frac{\partial\chi_j}{\partial y_{in}} = W + F_u \cos(\omega t). \tag{58}$$

This is a system of $(N + 2)$ second order, non-linear differential equations. There is an external radial force, which is allowed to act on the bearing system and no external mass is attached to the outer race. The "+" sign as subscript in these equations signifies that if the expression inside the bracket is greater than zero, then the rolling element at angular location θ_j is loaded giving rise to restoring force and if the expression inside bracket is negative or zero, then the rolling element is not in the load zone, and restoring force is set to zero. For the balanced rotor condition, the unbalance force (F_u) is set to be zero.

The deformation of spring at inner race χ_j (from Fig. 2) can be obtained as

$$x_{in} + \chi_j \cos\theta_x = x_{out} + \rho_j \cos\theta_j, \tag{59}$$

$$y_{in} + \chi_j \sin\theta_x = y_{out} + \rho_j \sin\theta_j. \tag{60}$$

From these two equations, the expression for χ_j is obtained as

$$\begin{aligned} \chi_j = &[(x_{out} - x_{in})^2 + \rho_j^2 + 2\rho_j(x_{out} - x_{in})\cos\theta_j \\ &+ 2\rho_j(y_{out} - y_{in})\sin\theta_j + (y_{out} - y_{in})^2]^{1/2}. \end{aligned} \tag{61}$$

Now the partial derivatives of χ_j with respect to ρ_j, x_{in} and y_{in} are

$$\frac{\partial\chi_j}{\partial\rho_j} = \frac{\rho_j + (x_{out} - x_{in})\cos\theta_j + (y_{out} - y_{in})\sin\theta_j}{\chi_j}, \tag{62}$$

$$\frac{\partial \chi_j}{\partial x_{in}} = \frac{(x_{out} - x_{in}) - \rho_j \cos\theta_j}{\chi_j}, \tag{63}$$

$$\frac{\partial \chi_j}{\partial y_{in}} = \frac{(y_{out} - y_{in}) - \rho_j \sin\theta_j}{\chi_j}. \tag{64}$$

The non-linear stiffness associated with point contact of spring for the inner and outer races is calculated by using Eq. (24) is

$$(k_{in}) = 7.055 \times 10^5 [\{r + \rho_r\} - \chi_j]^{1/2}, \tag{65}$$

$$(k_{out}) = 7.055 \times 10^5 [R - \{\rho_j + \rho_r\}]^{1/2}, \tag{66}$$

$$\frac{(\partial k_{in})}{\partial \rho_j} = -3.5725 \times 10^5 [\{r + \rho_r\} - \chi_j]^{-1/2} \frac{\partial \chi_j}{\partial \rho_j}, \tag{67}$$

$$\frac{(\partial k_{out})}{\partial \rho_j} = 3.5725 \times 10^5 [R - \{\rho_j + \rho_r\}]^{-1/2}. \tag{68}$$

2.5. Ball passage frequency

When the shaft is rotating, applied loads are supported by a few balls restricted to a narrow load region and the radial position of the inner race with respect to outer race depends on the elastic deflections at the ball to raceways contacts. Balls are deformed as they enter the loaded zone where the mutual convergence of the bearing races takes place and the balls rebound as they move to unloaded region. Time taken by shaft to regain its initial position is

$$t = \frac{\text{time for a complete rotation of cage}}{N_b}. \tag{69}$$

As the time needed for a complete rotation of the cage is $2\pi/\omega_{cage}$, the shaft will be excited at the frequency of $(N_b \times \omega_{cage})$ known as BPF.

Hence, BPF (ω_{bp}) is

$$\omega_{bp} = \frac{1}{2} N_b \omega_{inner} \left[1 - \frac{\rho_j}{R_p}\right] + \frac{1}{2} N_b \omega_{outer} \left[1 + \frac{\rho_j}{R_p}\right]. \tag{70}$$

Vibrations associated with the BPF are known as BPV or the elastic compliance vibrations. The effect of BPF can be worst when it coincides with a natural frequency of the shaft bearing system.

3. Results of the numerical simulations

The non-linear governing equations of motion (56)–(58) are solved by Newmark-β with Newton–Raphson method to obtain the displacements of the rolling elements and the shaft. In

order to study the effects of inner and outer race waviness in a more detail form, the shaft is assumed to be perfectly rigid and supported by two radial contact ball bearings. The numerical values of the parameters chosen for the numerical simulation are shown in Table 2. Numerical stability in the result is obtained by assuming 0.00001-radian angular rotation at each step. This causes a very large number of points. Therefore, every 400th point is plotted in the figures. To confirm the aperiodic behavior of the ball bearing model, the fast Fourier transformations are used. Balls are radially preloaded in order to ensure the continuous contact of all balls and the raceways, otherwise a chaotic behavior might be observed. The waviness amplitude was set to 2 μm and the number of waves round the races circumference is varied for a bearing with 8 balls (Figs. 4 and 5).

3.1. Outer race waviness

In order to observe the effect of number of waves, frequency domain vibrations of shaft-supported bearings are obtained as shown in Fig. 6. The shaft rotates at 2500 rpm.

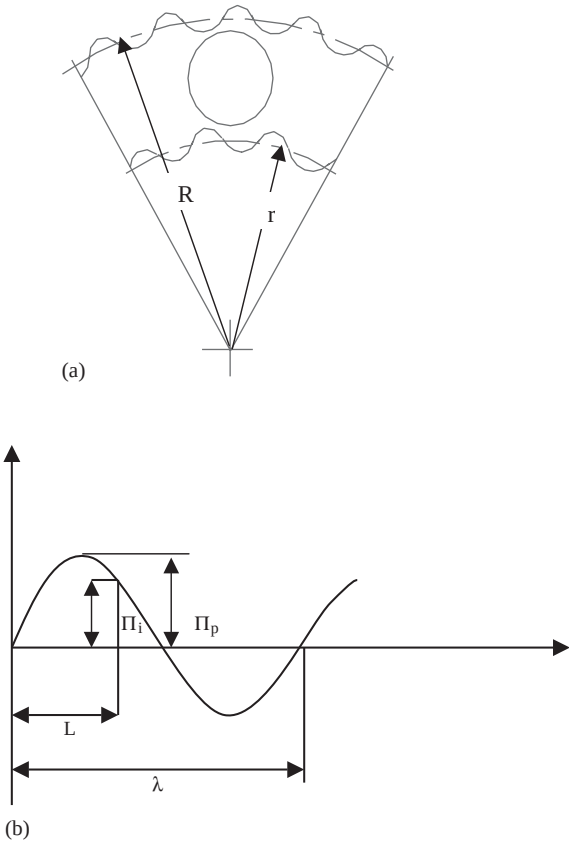

Fig. 4. (a) Waviness at the inner and outer races. (b) Wave of the race.

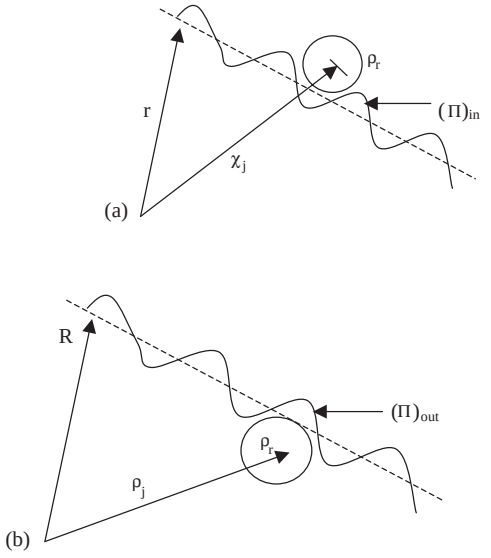

Fig. 5. (a) Contact between inner race and rolling element. (b) Contact between outer race and rolling element.

When the number of waves is 7, the peak amplitude of vibration appears at the BPF ($\omega_{bp} = 140$ Hz) as shown in Fig. 6a. The amplitude of peak is 3.5 μm. When the number of waves is 8, the dominant peak amplitude of vibration appears at the BPF with first superharmonic at twice of the BPF ($\omega_{bp} = 280$ Hz) as shown in Fig. 6b. The sever vibration occurs when the number of waves and balls are equals. The maximum noise occurs in this case and this is confirmed experimentally by Wardle [14]. Hence the sever vibration occur when the waviness order is $k = N_b$. When the number of waves is 12, peak amplitude of vibrations at twice of the BPF with first subharmonic at the BPF (ω_{bp}) as shown in Fig. 6c. When the number of waves is 16, the peak amplitude of vibrations appears at twice of the BPF ($\omega_{bp} = 280$ Hz) as shown in Fig. 6d. The amplitude of peak is 8 μm. A clear transformation from $q = 1$ to 2 can be observed in the obtained vibration spectrum. When the number of waves is 17, high amplitude of peak appears at twice of the BPF ($\omega_{bp} = 280$ Hz) as shown in Fig. 6e. The amplitude of peak is 15 μm.

Hence from the obtained results for outer race waviness, the sever vibrations occurs when the number of balls and waves are equal. The waviness order for sever vibration is $k = N_b$. It is observed from the obtained responses that small amplitude of waviness on the stationary outer race of a radial loaded bearing only produce vibration at frequencies that are harmonic of the ball to outer pass rate ($N_b \times \omega_{cage}$). The axial vibrations produced when the number of waves per circumference is an integral multiple of the number of balls in the bearing, which was experimentally proved by Wardle [14] and Yhland [11]. Table 3 summarizes the relevant waviness orders, their peak amplitudes and harmonic in the bearing spectrum.

3.2. Inner race waviness

The vibration produced by waviness on the rotating inner race exhibits a more complex spectrum than for outer race waviness. Axial vibration occurs at frequencies harmonic of the ball

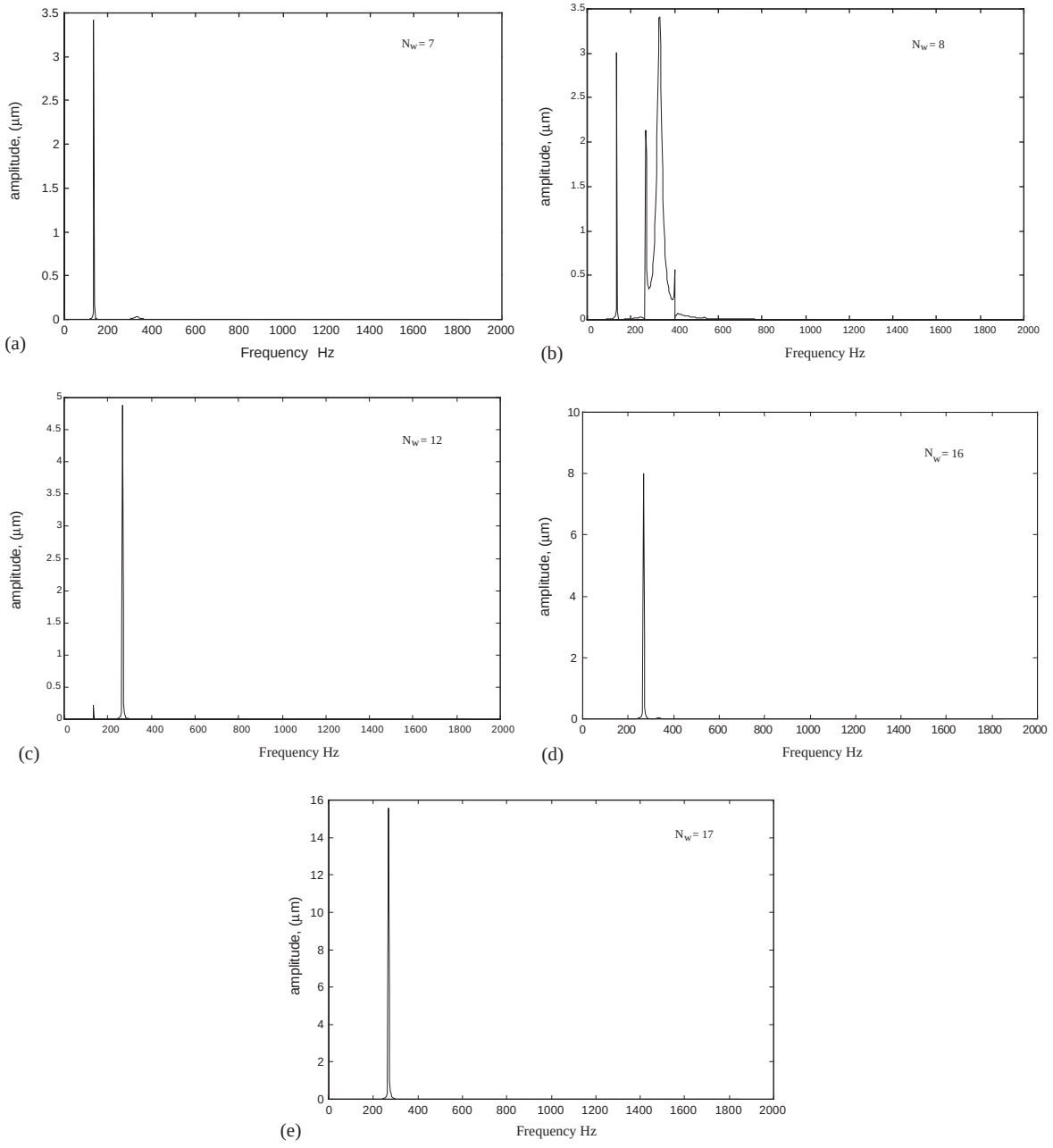

Fig. 6. (a–e) FFT of vibration due to outer race waviness of different orders ($N_b = 8$).

to inner pass rate $-N_b(\omega_{cage} - \omega)$. In order to study the inner race waviness, the bearings of the simulation model were assumed to have waviness in their inner race of the same order and magnitude such that both bearings are identical. The amplitude of the waviness was set to 2 μm.

Table 3
Summary of outer race waviness

Waviness order (lobes/circumference)	Peak amplitude (μm)	Harmonic in bearing spectrum
7	3.5	ω_{bp}
8	3.5	ω_{bp}
12	5	$2\omega_{bp}$
16	8	$2\omega_{bp}$
17	15	$2\omega_{bp}$

As inner race is fitted with the shaft, they rotate at the shaft speed. The vibration spectrums obtained for different waviness orders of inner race is shown in Fig. 7.

When the number of waves is 2, a dominant peak appears at 2ω (83 Hz) with the peaks at super harmonics of the shaft speed (135, 209, 270, 360 Hz) as shown in Fig. 7a. For the inner race waviness, wave passage frequency [$\omega_{wp} = N_b(\omega - \omega_{cage}) = 192$ Hz]. For the three waves, the peak amplitude appears at $\omega_{wp} + \omega$ (275 Hz) and at $\omega_{wp} - \omega$ (155 Hz). A peak with lower amplitude also appears at 3ω (125 Hz) as shown in Fig. 7b.

Now the waviness order and vibration frequency follow the formula as

$$\begin{array}{ll} \text{Waviness of orders} & \text{Vibration caused by waviness} \\ k = qN_b \pm p & qN_b(\omega - \omega_{cage}) \pm p\omega \end{array}. \tag{71}$$

When the number of waves is 5, the peak amplitude appears at $\omega_{wp} + 3\omega$ (320 Hz) where $q = 1$ as shown in Fig. 7c. The amplitude of peak is relatively very small (0.035 μm). When the number of waves is 7, the peak amplitude appears at $\omega_{wp} - \omega$ (155 Hz) where $q = 1$ and $p = 1$ as shown in Fig. 7d. The amplitude of peak is 2 μm. For 8 waves, the peak amplitude of vibration appears near to wave passage frequency (192 Hz) where $q = 1$ and $p = 0$ as shown in Fig. 7e. The amplitude of peak is 10 μm. When the number of waves is 9, the peak amplitude of vibration appears at $\omega_{wp} + \omega$ (235 Hz) where $q = 1$ and $p = 1$ as shown in Fig. 7f. The amplitude of peak is 7 μm. For 11 waves, the peak amplitude of vibration appears at $11(\omega - \omega_{cage}) + \omega$ (310 Hz) where $q = 1$ as shown in Fig. 7g. The amplitude of peak is 4 μm. When the number of waves is 12, the peak amplitude of vibration appears at $2\omega_{wp} - 4\omega$ (220 Hz) where $q = 2$ and $p = 4$ as shown in Fig. 7h. The peak amplitude is 1.8 μm. The other peaks appear at $\omega_{wp} + 2\omega$ (275 Hz), $\omega_{wp} - 2\omega$ (110 Hz) and at $\omega_{wp} + 4\omega$ (360 Hz). For 13 waves the peak amplitude of vibration appears at $2\omega_{wp} - 3\omega$ (265 Hz) where $q = 2$ and $p = 3$ as predicted from Eq. (71) shown in Fig. 7i. The peak amplitude is 0.2 μm. Other peak is at $\omega_{wp} + 3\omega$ (320 Hz). When the number of waves is 14, the peak amplitude of vibration appears at $2\omega_{wp} - 2\omega$ (306 Hz) where $q = 2$ and $p = 1$ as shown in Fig. 7j. The peak amplitude is 7.5 μm. For 15 waves the peak amplitude appears at $2\omega_{wp} - \omega$ (350 Hz) where $q = 2$ and $p = 1$ as shown in Fig. 7(k). The peak amplitude is higher 27 μm. For 16 waves the peak amplitude of vibration appears very near to $2\omega_{wp}$ (390 Hz) where $q = 2$ and $p = 0$. The peak amplitude is 15 μm. When the number of waves is 17, the peak amplitude appears at $2\omega_{wp} + \omega$ (430 Hz) where $q = 2$ and $p = 1$. The peak amplitude is 2.5 μm.

In the present results four different stages obtained. From $N_w = 2$ to 5, the less amplitude of vibration exist. From $N_w = 7$ to 9, the predicted vibrations are for $q = 1$in Eq. (71). From $N_w =$ 11 to 13, there is transformation from $q = 1$ to 2 in Eq. (71) and from $N_w = 14$ to 17 the predicted vibration is again for $q = 2$. The same trend for larger orders of waviness can be expected.

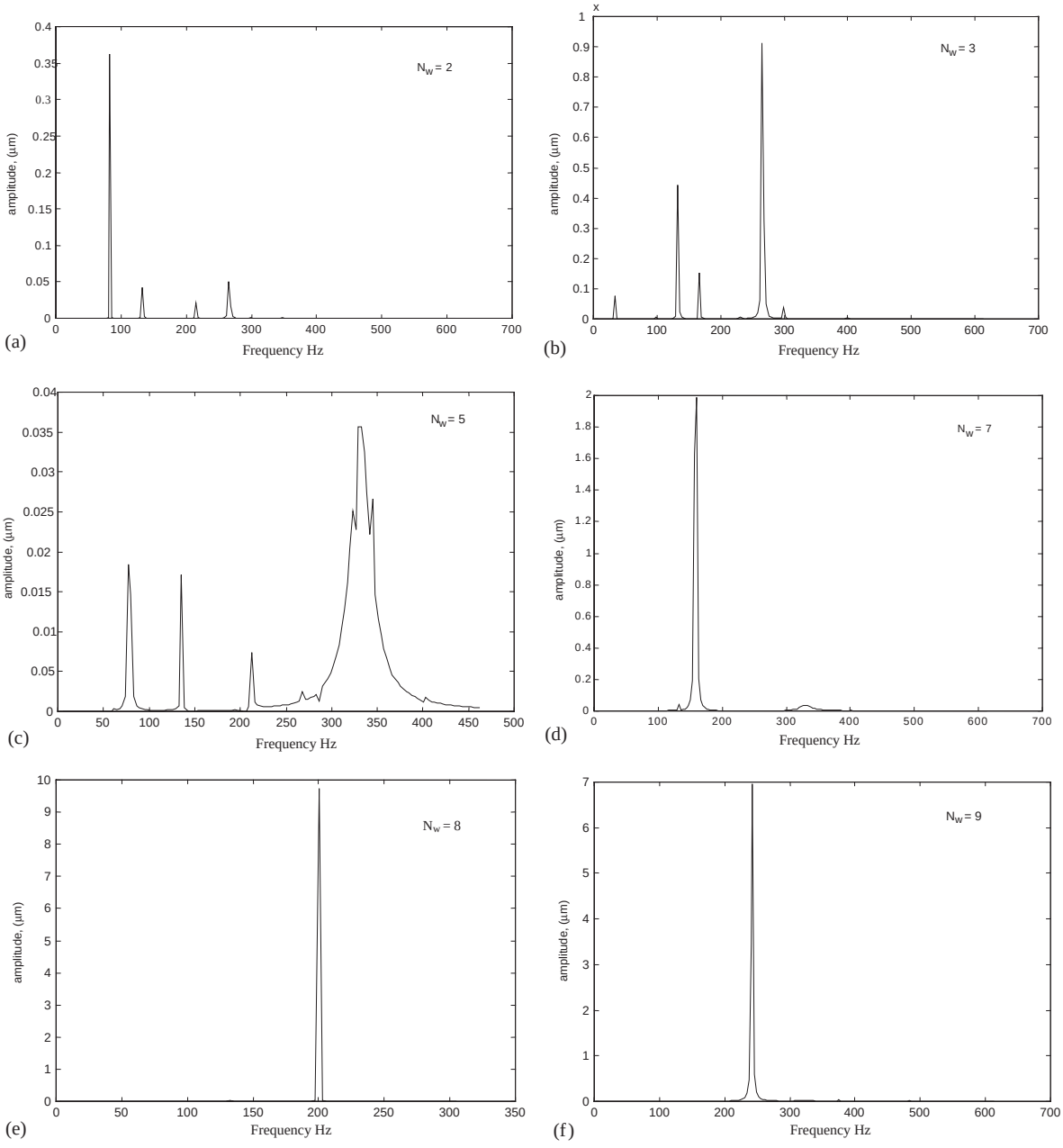

Fig. 7. (A–m) FFT of vibration due to inner race waviness of different orders ($N_b = 8$).

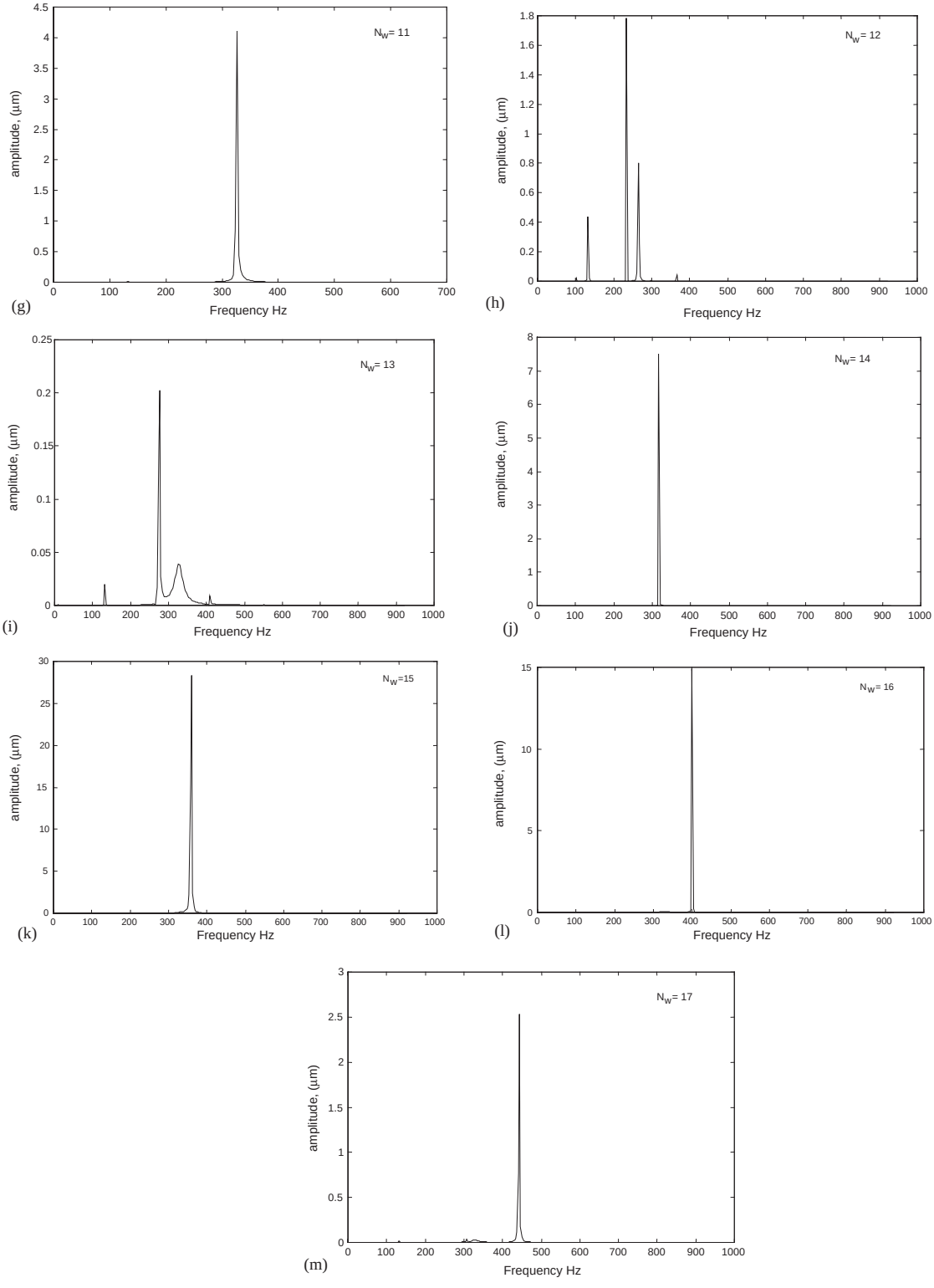

Fig. 7 (*continued*).

4. Conclusions

In the present investigation, an analytical model of a rotor bearing system has been developed to obtain the non-linear vibration response due to surface waviness in the races. From the obtained responses, it is implied that for the *outer race waviness*, the sever vibrations occurs when the number of balls and waves are equal. The waviness order for sever vibration is $k = N_b$. The axial vibrations appears at an integer multiple of the BPF $q(N_b \times \omega_{cage})$. The waviness order and vibration frequency for the outer race waviness are as follows:

$$\begin{array}{ll} \text{Waviness of orders} & \text{Vibration caused by waviness} \\ k = qN_b \pm p & qN_b\omega_{cage} \end{array}. \tag{72}$$

The analytical simulation presented in this paper confirms the experimental studies of other researchers. Because the load deflection relationship for balls is non-linear, in some cases Eq. (72) is only applicable to major peaks. In case of the *inner race waviness*, the peak amplitude of vibration follows the formula as given in Eq. (71) and the transformations of the peaks can be at $q\omega_{wp} \pm p\omega_{cage}$. For the waviness order *im*, peak amplitude of vibration and superharmonic appear at the wave passage frequency. Hence from this analysis the prediction about the major peaks at frequencies can be made.

Appendix A. Nomenclature

F_u	unbalance force, N
I	moment of inertia of each rolling element
I_{shaft}	moment of inertia of the shaft
I_{in}	moment of inertia of the inner race
I_{out}	moment of inertia of the outer race
k	waviness order
K	constant of proportionality, $N/mm^{3/2}$
L	arc length, mm
m_s	mass of the shaft, kg
m_{in}	mass of the inner race, kg
m_j	mass of the rolling elements, kg
m_{out}	mass of the outer race, kg
N_w	number of wave lobes
N_b	number of balls
p	empirical constant for a particular geometry
q	empirical constant for a particular geometry
R	radius of outer race, mm
r	radius of inner race, mm
r_{in}	position of mass center of inner race
r_{out}	position of mass center of outer race
T	kinetic energy of the bearing system
T_{shaft}	kinetic energy of the shaft

T_{i_race} kinetic energy of the inner race
T_{o_race} kinetic energy of the outer race
T_{roll_e} kinetic energy of the rolling elements
V potential energy of the bearing system
V_{shaft} potential energy of the shaft
V_{i_race} potential energy of the inner race
V_{o_race} potential energy of the outer race
V_{roll_e} potential energy of the rolling elements
V_{spring} potential energy of the springs
x_{in}, y_{in} center of inner race
x_{out}, y_{out} center of outer race
δ deformation at the point of contact at inner and outer race, mm
$(\dot{\phi})_{in}$ angular velocity of inner race
$(\dot{\phi})_{out}$ angular velocity of outer race
λ wave length, mm
ω_{cage} angular velocity of cage relating to the cage, rad/s
ω_{bp} ball passage frequency, Hz
ω_{wp} wave passage frequency, Hz
$(\Pi)_{in}$ amplitude of the wave at inner race, μm
$(\Pi)_{out}$ amplitude of the wave at outer race, μm
ρ_j radial position of the rolling element
ρ_r radius of each rolling element
θ_j angular position of rolling element
χ_j position of jth rolling element from the center of inner race
FFT fast Fourier transformation
BPF ball passage frequency, Hz
BPV ball passage vibration, Hz
WPF wave passage frequency, Hz

References

[1] H. Yamamoto, On the vibration of a shaft supported by bearing having radial clearances, *Transactions of Japan Society of Mechanical Engineers* 21 (1955) 182–192.
[2] O.G. Gustafson, T. Tallian, et al., Research report on study of the vibration characteristics of bearings, Reg: 585 14: 4223, December, Report: AL 631 023, 1963, SKF Ind. Inc.
[3] L.D. Meyer, F.F. Ahlgran, B. Weichbrodt, An analytical model for ball bearing vibrations to predict vibration response to distributed defects, *American Society of Mechanical Engineers Journal of Mechanical Design* 102 (1980) 205–210.
[4] E.H. Gad, S. Fukata, H. Tumara, Computer simulation of rotor radial vibration due to ball bearings, *Memories of the Faculties of Engineering, Kyushu universities* 44 (1984) 83–111.
[5] H.R. El-Sayed, Stiffness of deep-groove ball bearings, *Wear* 63 (1980) 89–94.
[6] H. Tamura, Y. Tsuda, On the spring characteristics of ball bearing (extreme characteristics with many balls), *Bulletin of Japan Society of Mechanical Engineers* 23 (1980) 961–969.
[7] V.B. Bal 'mount, E.B. Varlamov, I.G. Gorelik, Structural vibrations of ball bearings, *Soviet Machine Science* 1 (1987) 82–88.

[8] R.S. Sayles, S.Y. Poon, Surface topography and rolling element vibration, *Precision Engineering* 3 (3) (1981) 137–144.
[9] J. Datta, K. Farhang, A nonlinear model for structural vibrations in rolling element bearings: Part I—derivation of governing equations, *American Society of Mechanical Engineers Journal of Tribology* 119 (1997) 126–131.
[10] F.P. Wardle, S.Y. Poon, Rolling bearing noise, cause and cure, *Char. Mechanical Engineering* July/August (1983) 36–40.
[11] E.M. Yhland, A linear theory of vibration caused by ball bearings with form errors operating at moderate speeds, *American Society of Mechanical Engineers Journal of Tribology* 114 (1992) 348–359.
[12] N. Aktürk, The effect of waviness on vibrations associated with ball bearings, *American Society of Mechanical Engineers Journal of Tribology* 121 (1999) 667–677.
[13] N. Aktürk, M. Uneeb, R. Gohar, The effects of number of balls and preload on vibrations associated ball bearings, *American Society of Mechanical Engineers Journal of Tribology* 119 (1997) 747–753.
[14] F.P. Wardle, Vibration forces produced by waviness of the rolling surfaces of thrust loaded ball bearings, Part I: theory, *Proceedings of the Institution of Mechanical Engineers* 202 (C5) (1988) 305–312.
[15] T.A. Harris, *Rolling Bearing Analysis*, Wiley, New York, 1991.